Bilateral Adaptation of Longitudinal Control of Automated Vehicles and Human Drivers

Longxiang Guo[®] and Yunyi Jia[®]

Abstract-Automated vehicles have great potential to transform our existing transportation systems by improving driving safety, comfort, congestion, and emissions. Despite the tremendous efforts that have been spent on the development of various automated driving technologies, user acceptance of automated driving technologies is still low, which is largely caused by the gaps between automated driving controllers and human preferences. Recent research efforts have been focusing on adapting automated driving behaviors to human demonstrations. However, most existing methods assume that human demonstration is perfect and only focus on mimicking human driving behaviors. In reality, the human demonstration will not be ideal and will include some over-aggressive or over-conservative actions that compromise the safety or efficiency of the trained automated driving controller. In this paper, an Inverse Model Predictive Control (IMPC) based bilateral adaptation method for automated vehicles and human drivers is proposed. The method can adapt automated longitudinal driving behaviors to human preferences based on human interventions during automated driving. Meanwhile, it can also reject improper interventions and send warnings to the human driver such that he/she can realize the irrationality in his/her behaviors. Eventually, the automated driving controller will adapt to the human driver's preferences and the human driver will get rid of his/her bad driving habits. Human-in-the-loop experiments were conducted using a driving simulator to demonstrate the effectiveness of the proposed approach.

Index Terms—Human driving behaviors, inverse model predictive control, learning, and prediction.

I. INTRODUCTION

Automated driving technology has the potential of reducing traffic jams, increasing road and intersection capacity [1], [2], improving driving safety [3], and saving energy [4]. Tremendous efforts have been spent on various automated driving technologies to improve driving safety and comfort. However, according to multiple surveys about automated vehicles, user acceptance of automated vehicles is still low [5], [6]. A vital truth has been ignored that the technicalities of driving safety and comfort do not necessarily indicate the human perception of safety and comfort. Human perceived safety and comfort are usually subjective. For instance, a certain time headway, which lies within the technically safe range, may cause conservative drivers to feel nervous and unsafe, but at the same time, cause aggressive drivers to feel impatient and uncomfortable. This research gap indicates that technology-focused research efforts fail to put humans into consideration or in the loop of automated vehicle planning and control, which consequently limits the user acceptance of automated vehicles.

To address this problem, many recent research works propose to adapt automated vehicles to human drivers. The adaptation of automated vehicles refers to the process of adjusting automated

Manuscript received 14 April 2021; revised 22 November 2021, 5 May 2022, 1 November 2022, and 22 December 2022; accepted 23 January 2023. Date of publication 17 February 2023; date of current version 8 May 2023. This work was supported in part by the National Science Foundation under Grant CNS-1755771 and Grant IIS-1845779. The Associate Editor for this article was H. Park. (Corresponding author: Yunyi Jia.)

The authors are with the Department of Automotive Engineering, Clemson University, Greenville, SC 29607 USA (e-mail: longxig@clemson.edu; yunyij@clemson.edu).

Digital Object Identifier 10.1109/TITS.2023.3242278

driving parameters to achieve some desired driving behaviors. Some vehicles have already provided interfaces for human drivers to manually adjust several control parameters, such as speed in cruise control and speed and headway in adaptive cruise control. But these simple parameters are far from enough to represent human driving preferences. This paper focuses on the adaptation of longitudinal behaviors of automated vehicles and human drivers. Related research works have attempted to automatically learn and adapt these control parameters for automated vehicles, and many of them have been using car-following models such as the Tampère (TMP) model [7], Optimal Velocity Model (OVM) [8], and Intelligent Driver Model (IDM) [9]. The parameters of these models are identified based on human demonstrations. The limitations of these models are their simple structure and an insufficient number of parameters, which make them unsuitable for adapting to an individual human driver. In recent years, many data-driven machine learning approaches have been proposed to learn the behaviors of a human driver. The most popular ones are the Artificial Neural Network (ANN)-based approaches [11], [12], [13], [14], [15], [16]. However, these approaches require a large set of carefully prepared data to train the network parameters.

The existing unidirectional adaptation approaches for automated driving models adapt automated vehicles to human drivers in order to purely mimic human driving behaviors, which may also mimic some poor human driving behaviors. Thus, an adaptation method that can resist such undesired human demonstration is needed. Also, it is equally important to adapt the human driver such that he/she can give up the expectation of undesired driving behaviors in order to improve user acceptance. However, the related research is quite limited. Existing research has shown that automated driving functions can send audio, visual, and haptic signals to human drivers when their attention is needed [17], [18] and that human drivers change their driving behaviors in response to such feedback from automated driving functions [19]. Most research works have focused on the short-term transient behaviors of human drivers in ad-hoc ways after they receive the signals as reminders to ensure the safe operation of automated driving functions [21], [22]. Few have focused on the change in human long-term driving styles. Moreover, most of these works do not have a theoretical model to support how this feedback influences human drivers. Few have studied using warning feedback to change human long-term driving styles and expectations on automated driving behaviors and subsequently influence human interventions on automated vehicles. Therefore, creating intuitive feedback from automated vehicles to humans to change their driving styles and their expectations of the behaviors of automated vehicles, and generating appropriate human intervention data to adapt the controls of automated vehicles are of great research value.

Using soft constraints is a popular method in optimization [23] and optimal control [24], [25] for increasing feasibility. Despite their popularity, soft constraints are mainly used for control purposes. Few studies have used them to learn the driving control models, which is an inverse problem of controls. Our previous works [26], [27], [28] have proposed an inverse model predictive control (IMPC) based modeling method for the longitudinal motion of human-driven

1558-0016 © 2023 IEEE. Personal use is permitted, but republication/redistribution requires IEEE permission. See https://www.ieee.org/publications/rights/index.html for more information.

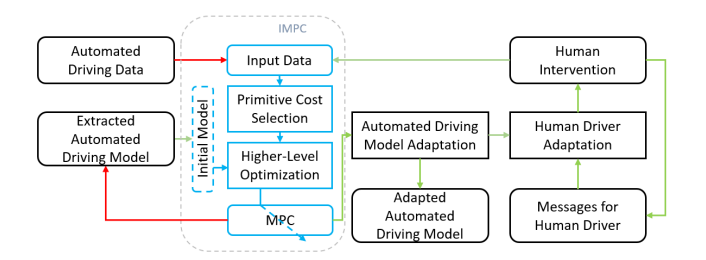


Fig. 1. Framework of bilateral adaptation mechanism.

vehicles. Hence, integrating soft constraints into our proposed IMPC to learn the driving models is worth studying. The IMPC proposed in our previous work was mainly used for the prediction of human-driven vehicles' trajectories. This work further extends the method to the modeling of automated driving behaviors and the adaptation of the automated driving model based on human interventions, which is new and different from our previous work. The major contributions are summarized as follows.

- Proposing a new bilateral adaptation framework for both automated vehicles and human drivers. The framework first extracts the models of automated driving vehicles based on our proposed IMPC approach. It then builds on these models to adapt the automated driving behaviors according to human interventions and also adapt human expectations on automated driving by incorporating safety and efficiency constraints and intuitive warning feedback.
- Designing and conducting human-in-the-loop automated driving experiments to validate that the proposed bilateral adaptation framework can adapt both automated driving controllers and human expectations on automated vehicles without causing safety hazards and compromising efficiency.

The rest of the paper is organized as follows. Section II introduces the details of the bilateral adaptation mechanism. Section III presents the experimental design and the analysis of the results.

II. BILATERAL ADAPTATION OF AUTOMATED VEHICLES AND HUMAN DRIVERS

In this section, the framework for the bilateral adaptation mechanism is described in II-A. The details of IMPC-based automated driving model extraction and adaption are introduced in II-B and II-C respectively. The method for adapting human drivers is presented in II-D

A. Framework for Bilateral Adaptation

In this paper, we separate the bilateral adaptation mechanism into two steps. The first step is the construction and adaptation of the automated driving model, while the second step is the adaptation of human drivers. The structure of the bilateral adaptation mechanism is shown in Fig. 1. The lines with different colors in the figure represent the information transfer in different processes.

Given an automated vehicle, it is important to know how it drives before performing any adaptation. We propose to learn the automated driving model of an automated vehicle from its real-time driving data. In this paper, we choose to construct a generic automated driving control model in the form of model predictive control (MPC) using the IMPC method that we proposed before. The IMPC method has been shown to be effective in modeling human drivers' longitudinal driving behaviors. In this paper, we are extending the application field of the IMPC method to the modeling of a generic automated driving controller. The cost function of MPC will be core to describe the behaviors of an automated vehicle. For different automated vehicles,

their cost functions will be different. After the model of the automated vehicle is obtained, it is adapted to the human driver's preferences using the driver's intervention data during automated driving. IMPC approach is applied here again to complete the adaptation of the automated driving model.

During the adaptation, if improper human interventions are detected, the vehicle will inform the human driver about the situation such that the human driver can eventually avoid similar improper interventions. Meanwhile, the IMPC will penalize the cost functions that cause the vehicle to drive in an unsafe or inefficient way such that the adapted automated driving model is not affected by those improper human interventions.

B. Extraction of Automated Driving Model

The purpose of this model extraction is to turn any generic automated driving controller into a unified form that is proven to be effective in modeling a human driver. In this paper, we chose to use IMPC to extract the automated driving model to a model predictive controller. Since the details of IMPC have been included in our previous papers [26], [27], [28], this section will only provide a brief description of the IMPC.

The IMPC utilizes the cost function in MPC to represent a controller's driving preferences. IMPC finds the best primitive costs to be included in the cost function and identifies the weights and the references of those primitive costs to formulate the most suitable cost function dedicated to the controller.

The vehicle motion model (1) used by IMPC is a linear time-invariant (LTI) model with a first-order lag with a time constant τ [29], where a_a is the ego automated vehicle's acceleration, v_a is its speed, s_a is the travelled distance, and u_a is the control intput.

$$\begin{bmatrix} \dot{s_a} \\ \dot{v_a} \\ \dot{a_a} \end{bmatrix} = \begin{bmatrix} 0 & 1 & 0 \\ 0 & 0 & 1 \\ 0 & 0 & -\frac{1}{\tau} \end{bmatrix} \begin{bmatrix} s_a \\ v_a \\ a_a \end{bmatrix} + \begin{bmatrix} 0 \\ 0 \\ \frac{1}{\tau} \end{bmatrix} u_a \tag{1}$$

The MPC problem can be formulated by a constrained optimization problem that minimizes the cost function J_a over the prediction horizon:

$$u_{a}^{*} = \arg \min_{u_{a}} J_{a}$$

$$s.t. -10m/s^{2} \le a_{a} \le 5m/s^{2}$$

$$0 \le v_{a} \le 40m/s$$

$$-10m/s^{2} \le u_{a} \le 5m/s^{2}$$

$$d_{a} \ge 1.5m$$
(2)

These basic constraints are introduced to ensure the feasibility and rationality of the MPC controller. The MPC also requires another model for the lead vehicle, which is as follows:

$$\begin{bmatrix} \dot{s}_l \\ \dot{v}_l \end{bmatrix} = \begin{bmatrix} 0 & 1 \\ 0 & 0 \end{bmatrix} \begin{bmatrix} s_l \\ v_l \end{bmatrix} + \begin{bmatrix} 0 \\ 1 \end{bmatrix} a_l \tag{3}$$

where a_l is the lead vehicle's acceleration, v_l is its speed, s_l is its traveled distance. This facilitates the calculation of the headway distance $d_a = s_l - s_a$ over the prediction horizon.

The cost function J_a is further expressed as:

$$J_a = \sum \Omega_a^T \Phi_a \tag{4}$$

where $\Phi_a = (\phi_1, \phi_2, ...)^T$ is a set of primitive costs for the humandriven vehicle and $\Omega_a = (\omega_1, \omega_2, ...)^T$ is a set of associated weights. A primitive cost ϕ_j is shown in (5), where k is the number of the current time step, N is the number of prediction steps, and r_j is the target value of the motion states y_j . Note that motion states can be the ego vehicle's speed, look-ahead distance gap and control inputs, etc.

$$\phi_j = g(x_h, x_a, r_j, u_h) = \sum_{k=-k}^{k+N} (y_j(\kappa) - r_j)^2$$
 (5)

The primitive costs are used independently as stand-alone cost functions, which can be written as:

$$J_{\phi_j} = \phi_j = \sum_{\kappa=k}^{k+N} (y_j(\kappa) - r_j)^2$$
 (6)

and then the reference r_j is learned with a higher-level optimization (7). In (7), E is the evaluation error of the MPC over an automated driving demonstration, and C_{r_j} is the admissible set for r_j . When the higher-level optimization finishes, a minimum prediction error E_{ϕ_j} over demonstrations will be obtained for the primitive cost ϕ_j .

$$r_j^* = \arg \min_{r_j} E$$

$$s.t. : r_j \in C_{r_j}$$
(7

If the controller is focusing on ϕ_j and trying to maintain y_j at a specific target value during driving, the resultant E_{ϕ_j} should be small. This means that ϕ_j can be a 'good' primitive cost in the final cost function. Otherwise, the resulted E_{ϕ_j} should be large, and ϕ_j might better be excluded from the cost function. All primitive costs are then ranked based on their E_{ϕ_j} values. We assume that $\Phi_a^* = (\phi_1^*, \phi_2^*, \dots, \phi_j^*)^T$ is the set of all available primitive costs that have been ranked from good to bad, with ϕ_1^* being the best and ϕ_j^* being the worst. Followed by this, we propose to formulate the cost function by combining the primitive costs from 'good' to 'bad', which can be described by (8).

$$J_{1} = \omega_{1}\phi_{1}^{*},$$

$$J_{2} = \omega_{1}\phi_{1}^{*}, +\omega_{2}\phi_{2}^{*},$$

$$J_{3} = \omega_{1}\phi_{1}^{*}, +\omega_{2}\phi_{2}^{*}, +\omega_{3}\phi_{3}^{*}...$$

$$J_{i} = \omega_{1}\phi_{1}^{*}, +\omega_{2}\phi_{2}^{*} + ... + \omega_{i}\phi_{i}^{*}$$
(8)

Since a controller normally focuses on more than one aspect during driving, it is reasonable to skip J_1 and start with a combination of the top two or three best primitive costs in the cost function first. Subsequently, in the following attempts, the next best primitive cost is added to the cost function. Every cost function J_j will learn its parameters using the higher-level optimization. Denoting the set of references $r_1 \dots r_j$ by R_j , and the set of weights $\omega_1 \dots \omega_j$ by Ω_j , the optimization can be expressed as:

$$(\Omega_j^*, R_j^*) = \arg \min_{\Omega_a, R} E$$

$$s.t. : \Omega_j \in C_{\Omega_j}, R_j \in C_{R_j}$$
(9)

where C_{Ω_j} and C_{R_j} are the admissible sets for Ω_j and R_j respectively. The total error E is reduced by optimizing the weights Ω_j and the references R_j in the cost function. Since only the relative values of the weights are important, it is practical to fix a weight to 1 and optimize the rest [31]. The objective function of this higher-level optimization is yet another optimization problem, however, the Jacobian of E is not obtainable. Thus, the Pattern Search (PS) algorithm [32] is adopted in this paper. Each cost function I_j will get a minimal evaluation error E_j from the higher-level optimization. Adding an effective primitive cost ϕ_j should reduce the error E_j while adding an ineffective primitive cost will not bring any benefit but affect the optimization convergence, which will result in a larger evaluation error. Thus, the addition of primitive costs will be repeated until the evaluated performance of the predictor starts to

deteriorate. At this point, the previous cost function can be selected to be the best cost function. It has been shown that the proposed method to select the cost function is very effective, and the best cost function in this paper is chosen to be (10), where v_r is the relative speed between the ego vehicle and the lead vehicle, and $TTCi = v_r/d_a$ is the time to collision inverse. The three other primitive costs that have been evaluated but excluded from the cost function are the time headway inverse $THWi_a = v_a/d_a$, the headway distance d_a , and the ego vehicle speed v_a .

$$J_{a} = \sum_{\kappa=k}^{k+N} \left[\omega_{a}(a_{a}(\kappa) - a_{a}^{ref})^{2} + \omega_{v}(v_{r}(\kappa) - v_{r}^{ref})^{2} + \omega_{TTCi}(TTCi_{a}(\kappa) - TCCi_{a}^{ref})^{2} + \omega_{u}(u_{a}(\kappa) - u_{a}^{ref})^{2} \right]$$

$$(10)$$

C. Adaptation of Automated Driving Model

After the automated driving model has been extracted, it is adapted to the human drivers' preferences using human intervention data collected during automated driving. The IMPC process given in II-B is repeated by using the human intervention data instead of the automated driving data as the demonstration. However, in order to avoid the negative impacts caused by improper human interventions, the higher-level optimization step (10) needs to be modified to accommodate this extra requirement. Directly adding stricter hard constraints to (2) can make sure the controller does not violate any safety or efficiency requirements. However, doing such will completely change the rank of the primitive costs and even cause feasibility issues during the higher-level optimization process. Thus, instead of adding hard constraints to the MPC, we chose to add soft constraints to the higher-level optimization, and hence, (9) turns into (11):

$$\left(\Omega_{j}^{*}, R_{j}^{*}\right) = \arg\min_{\Omega_{a}, R} E + P$$

$$s.t.: \Omega_{j} \in C_{\Omega_{h}}, R_{j} \in C_{R}$$
(11)

P is a set of performance constraints p_n :

$$P = \sum_{n=1}^{N} \omega_n \sum_{m=1}^{M} p_n(m) t_s$$
 (12)

where M is the total number of data points of each evaluation, t_s is the sample time, and ω_n is the weight for different performance constraints. Each performance constraints $p_n(m)$ is further detailed as follows:

$$p_n(m) = \begin{cases} 0, & x(m) meets the requirements \\ p, & otherwise \end{cases}$$
 (13)

where p is a positive penalty value

D. Adaptation of Human Driver

In the previous step, we propose to adapt the automated vehicles according to human interventions, driving performance, and human-perceived safety and comfort levels. In this second step, we also propose to take appropriate adaptation measures to make humans aware of their improper behaviors when their intervention will make the automated driving performance worse, and eventually correct them.

While the human driver is experiencing automated driving, he/she can take over the control of the vehicle by directly operating the brake or throttle pedals. The automated driving will be resumed by pressing a button on the steering wheel. During the intervention, the necessary data is recorded for the adaptation of the automated



Fig. 2. The safety warning light (left) and the efficiency warning light (right) for the human driver during intervention.

driving model, and the driver's performance is monitored. The same performance constraints in (13) are evaluated in real-time during human interventions. If any of the constraints is violated, then the intervention is considered to be harmful to the driving performance.

```
Algorithm 1 Bilateral Adaptation Process
  while automated driving
      if no human intervention do
         collect vehicle state data
         extract automated driving model
      else
          if intervention is making vehicle unsafe do
             display red alarm light
             play rapid siren
          else if intervention is making vehicle inefficient do
                display yellow reminder light
                play gentle beep sound
          end
             collect intervention data
             adapt automated driving model
      end
  end
```

When that situation happens, proper feedback needs to be provided to the human driver to let him/her be aware of the improper behaviors. Such feedback is provided in the form of resistant force feedback generated on the accelerator and brake pedals in addition to conventional alarm signals such as sounds and lights. In this paper, the simulator will display red alarm lights and play a rapid siren to the driver when the safety constraints are violated and display a yellow reminder light, and play a gentle beep sound to the driver. The warning interface is shown in Fig. 2. The human drivers will learn from the feedback information and eventually stop improper intervention during automated driving. The entire bilateral adaptation process including the adaption of the human driver is given in Algorithm 1. This process is repeated until the human driver's intervention percentage drops to or close to zero during a long enough automated driving experience.

III. EXPERIMENTAL RESULTS AND ANALYSIS

In this section, the experimental results and analysis are presented. The setup of the experimental environment is introduced in III-A. The result of the automated driving model extraction is presented in III-B. The bilateral adaption results of an aggressive driver and a conservative driver are discussed in III-C and III-D respectively.

A. Experiment Setup

In this paper, the experiment is conducted using a 3D real-time driving simulator with motion feedback. It has been shown that a well-designed driving simulation can produce results close to reality. Our simulation was carefully designed with realistic driving scenarios



Fig. 3. Real-time 3D simulation with motion feedback.

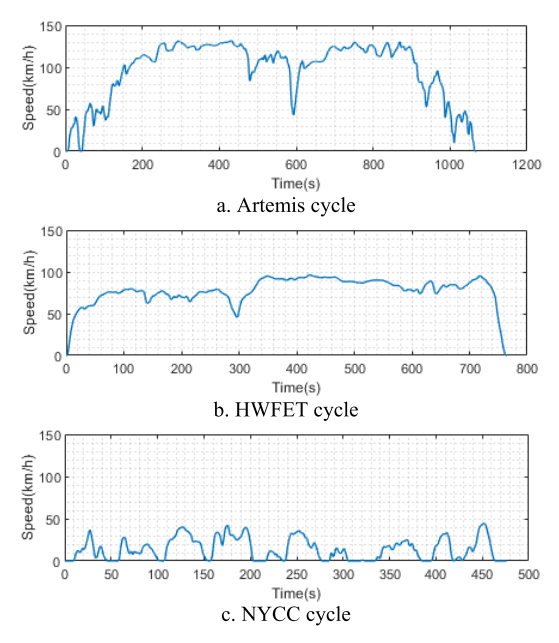


Fig. 4. Speed profiles of different cycles a. Artemis cycle b. HWFET cyclec. NYCC cycle.

including an accurate vehicle dynamics model, high-quality vehicle 3D model, and high-fidelity feedback such that the influence of the difference between the simulation model and the real-life vehicle could be minimized.

The simulator used in this paper is shown in Fig. 3. There are two vehicles in the simulation. The lead vehicle is an automated vehicle that tracks a cycle that is merged from three standard driving cycles. The first one is the EPA Highway Fuel Economy Test Cycle (HWFET) [33], which is a 12-minute-long mild highway cycle. The second is the Artemis Motorway 130 cycle [34] which is an 18-minute-long aggressive motorway cycle with heavier braking and wider open throttle. The last one is the New York City Cycle (NYCC) [33] with shortened stop time, which is an eight-minute-long urban driving cycle. These three cycles provide a variety of different driving behaviors for the experiment. The longitudinal motion model of this vehicle is a kinematic model that takes speed as an input.

The rear vehicle is the ego vehicle to be controlled by either an MPC controller or a human driver in real time. The motion model of this vehicle is a longitudinal dynamics model that considers air resistance, rolling resistance, and the inertia of the vehicle body and the wheels. The model takes torque at wheel as the input. When this vehicle is controlled by a human driver, the signals from the brake and throttle pedals are transformed into torque at the wheel's request directly. Both positive torque (throttle) and negative torque (brake) signals pass through a first-order lag element to simulate the response time in the powertrain and brake systems. The powertrain system has a larger time constant of $\tau_p = 0.45s$, and the brake system has a smaller time constant of $\tau_b = 0.1s$. When this vehicle is driven by

an MPC, the desired acceleration generated by the MPC is converted to torque at wheel by using a PI controller.

During automated driving, human intervention is triggered if the human's torque request has a different sign from the MPC's torque request, or if it has a larger amplitude. In both the learning and the testing phases, the prediction horizon of MPC was chosen to be 10 seconds, and the prediction step size Δt_P was chosen to be 0.5 seconds. The control frequency was 20Hz. In this paper, the MPC problem is solved using the ACADO toolkit [35].

B. Automated Driving Model Extraction

In this section, the result of the automated driving model extraction is presented. The Tampère (TMP) [7] cruise controller is selected as the generic automated longitudinal controller:

$$u_a = k_1(v_l - v_a) + k_2(d - d_{desired})$$
 (14)

where k_1 and k_2 are the tunable weights, d is the current headway distance, and $d_{desired}$ is the desired headway distance, which is calculated by:

$$d_{desired} = d_{min} + THW_{desired}v_a \tag{15}$$

where d_{min} is the minimum allowed safety distance and $THW_{desired}$ is the desired time gap. In the experiment, k_1 and k_2 were chosen to be 2 and 0.8 respectively, and d_{min} was chosen to be 1.5m, which is the same as the minimum allowed headway distance of the MPC controller. $THW_{desired}$ was chosen to be 0.7s. Such values were selected based on our experience in our previous work [33] to mimic a neutral driving style. The IMPC-based model extraction method was applied to the TMP controller, and the result is shown in Fig. 5. From the figure, it is seen that the extracted controller is maintaining almost the same headway distance as the original TMP controller. This implies that the IMPC method is effective in extracting automated driving models from the generic longitudinal controller.

C. Bilateral Adaptation of Aggressive Driver and Automated Driving Controller

In this section, an aggressive driver was required to experience the extracted automated driving model using the driving simulator and intervene if he/she was uncomfortable in real-time. After the extracted model has completed a merged cycle, the intervention data collected from the human driver is used for the first round of adaptation. During the adaptation, safety cost (16) is used to mitigate the negative influence of over-aggressive interventions. Designing p_n in this form penalizes the cost function if THW is too small, and the penalty accumulates over time. The training process reduces the value and lasting time of THW which breaks the safety limit.

In our previous work [33], the most aggressive driver maintained an average THW of 0.67s. In [34], the automated cruise control caused string instability when maintaining a time headway lower than 0.6s, and was barely maintaining string stability when the time headway was 0.7s. Thus, a THW smaller than 0.6s is considered dangerous and aggressive for both human drivers and autonomous controllers. A THW threshold of 0.5s for over-aggressive interventions is selected in this paper.

$$p_n(m) = \begin{cases} 0, & THW > 0.5s \\ \int (THW^{-1} - 2)dt, & otherwise \end{cases}$$
 (16)

After the first round of adaptation is finished, the human driver will experience the adapted model controlling the vehicle to follow the lead vehicle again and intervene if he/she feels necessary.

TABLE I
AUTOMATED DRIVING MODEL ADAPTION
RESULT FOR AGGRESSIVE DRIVER

Drive Cycle	Adaptation	Average THWi (s ⁻¹)	Maximum THWi (s^{-1})	Maximum Spacing (m)	Minimum Spacing (m)
HWFET	Original	1.04	1.11	24.14	4.85
	1st Adapt.	1.66	1.89	14.29	5.00
	2 nd Adapt	1.69	1.92	14.04	5.01
Artemis	Original	1.10	1.26	33.33	4.78
	1st Adapt.	1.74	2.03	21.08	4.78
	2 nd Adapt	1.75	2.03	21.07	4.76
NYCC	Original	0.53	0.96	12.81	4.68
	1st Adapt.	0.46	1.15	11.16	4.44
	2 nd Adapt	0.46	1.17	11.10	4.40

 $\label{eq:table-ii} \textbf{TABLE II}$ $\mbox{Human Intervention Percentage} - \mbox{Aggressive Driver}$

Original Model	After 1st Adaptation	After 2 nd Adaptation
70.03%	45.85%	0%

The automated driving model is then adapted using the second round of intervention data with the same safety cost in (16). This process is repeated until the human intervention percentage drops to or close to zero. The adaptation results of the automated driving controller are shown in Fig. 6 and TABLE I. The intervention percentage of the human driver in every intervention iteration is shown in TABLE II

Fig. 6 shows that the extracted original driving model was trying to keep a time gap of 0.7 seconds. The aggressive driver tried to maintain a time headway that was shorter than 0.7 seconds most of the time. By using the aggressive training data to adapt the driving model, the model after the first adaptation was able to maintain a much shorter headway distance than the original model. TABLE I shows that both the average and maximum THWi increase. In other words, the time gap decreases significantly after the first adaption. Meanwhile, due to the existence of penalty (16) in the higher-level optimization, the adapted driving model never went below the safety time headway constraint of 0.5 seconds. As shown in TABLE I, the maximum THWi stays below or around 2.0 most of the time. However, in the Artemis cycle, the maximum THWi is slightly above 2.0 to 2.03, which is caused by the difference between the motion model used by the MPC and the motion model of the vehicle. After the first round of adaptation, the human driver still felt uncomfortable and intervened during the 2nd round of automated driving experience, although the intervention percentage dropped massively from 70.03% to 45.85%. After training the driving model with the 2nd round of intervention data, the performance of the model only changed a little bit since the driving model in the first round of adaptation was already approaching the safety constraint. Although the 2nd round of adaptation did not make big changes to the automated driving controller, it reduced the intervention rate from 45.85% to 0% since the human driver kept receiving warnings during the 2nd round of intervention. Overall, the proposed bilateral adaptation mechanism was able to adapt the automated driving controller to human preferences without creating safety hazards, while correcting the human driver's over-aggressive driving habits.

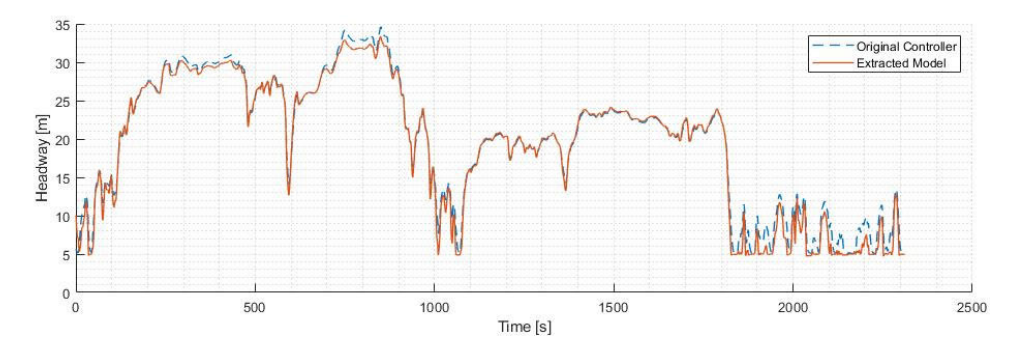


Fig. 5. Result of the TMP model extraction.

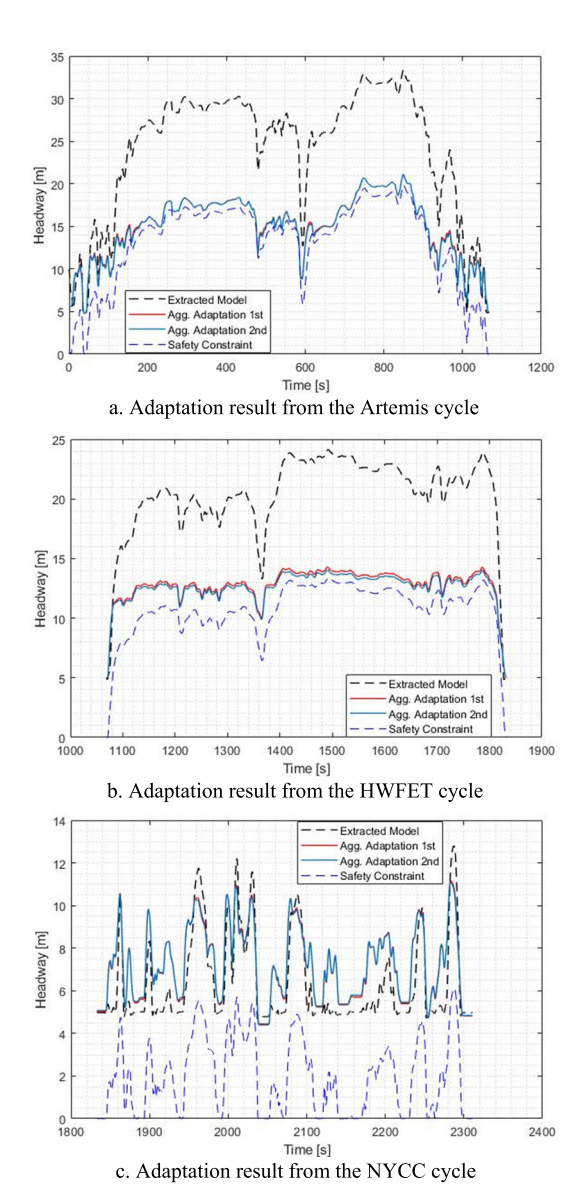


Fig. 6. Adaptation result of the aggressive driver a. Adaptation result from the Artemis cycle b. Adaptation result from the HWFET cycle c. Adaptation result from the NYCC cycle.

D. Bilateral Adaptation of Conservative Driver and Automated Driving Controller

In this section, a conservative driver was required to experience the extracted automated driving model using the driving simulator and intervene if he/she was uncomfortable in real-time. During the

TABLE III
AUTOMATED DRIVING MODEL ADAPTION RESULT
FOR CONSERVATIVE DRIVER

Drive Cycle	Adaptation	Average THWi (s ⁻¹)	Maximum THWi (s ⁻¹)	Maximum Spacing (m)	Minimum Spacing (m)
HWFET	Original	1.04	1.11	24.14	4.85
	1st Adapt.	0.81	0.84	32.50	4.86
	2 nd Adapt	0.81	0.84	32.53	4.86
Artemis	Original	1.10	1.26	33.33	4.78
	1st Adapt.	0.80	0.85	48.29	4.81
	2 nd Adapt	0.80	0.84	48.23	4.81
NYCC	Original	0.53	0.96	12.81	4.68
	1st Adapt.	0.50	0.85	14.81	4.73
	2 nd Adapt	0.50	0.84	14.81	4.73

TABLE IV
HUMAN INTERVENTION PERCENTAGE – CONSERVATIVE DRIVER

Original Model	After 1st Adaptation	After 2 nd Adaptation
64.37%	17.21%	0%

adaptation, efficiency cost (17) is used to mitigate the negative influence of over-conservative interventions. Similarly, designing p_n in this form will penalize the cost function if THW is too big, and the penalty accumulates over time. The training process will try to increase the value and reduce the lasting time of THW that breaks the efficiency limit.

Existing work [35] suggests that the THW of most human drivers lies between 1 second and 2 seconds. A THW threshold of 1.1 seconds for over-conservative interventions is selected such that the automated controller can increase road capacity compared to the human drivers after adaption.

$$p_n(m) = \begin{cases} 0, & THW < 1.1s \\ p, & otherwise \end{cases}$$
 (17)

Similar to the aggressive driver experiment, after the first round of adaptation is finished, the conservative driver will experience the adapted model controlling the vehicle to follow the lead vehicle again and intervene if he/she feels necessary. The automated driving model is then adapted using the second round of intervention data with the same safety cost (17). This process is repeated until the human

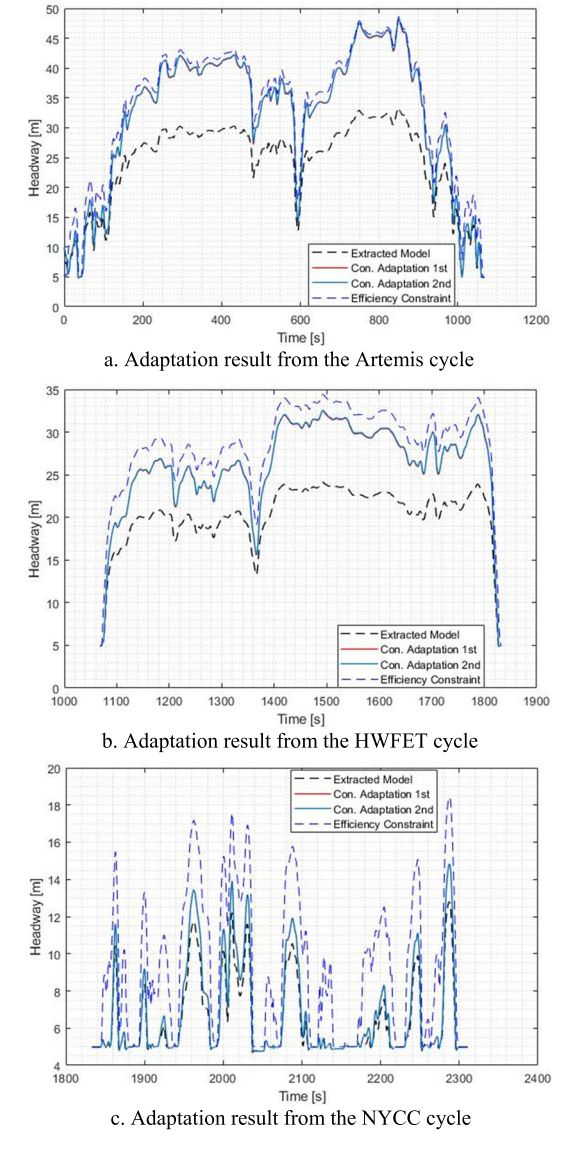


Fig. 7. Adaptation result of the conservative driver a. Adaptation result from the Artemis cycle b. Adaptation result from the HWFET cycle c. Adaptation result from the NYCC cycle.

intervention percentage drops to or close to zero. The adaptation results are shown in III-E and TABLE III. The intervention percentage of the human driver in every intervention iteration is shown in TABLE IV.

Fig. 7 shows that the extracted original driving model was trying to keep a time gap of 0.7 seconds. The conservative driver tried to maintain a time headway that was greater than 1.1 seconds most of the time. By using the conservative training data to adapt the driving model, the model after the first adaptation was able to maintain a much longer time gap than the original model. Meanwhile, due to the existence of penalty (17) in the higher-level optimization, the adapted driving model never went beyond the efficient time headway constraint of 1.1 seconds. As shown in TABLE III, the average and maximum THWi decrease while the maximum spacing increases a lot after the first round of adaption, indicating that the automated driving model is catching the conservative driving behavior of the human driver from the intervention. After the first round of adaptation, the human driver still felt uncomfortable and intervened during the 2nd round of automated driving experience, although the

intervention percentage dropped massively from 64.37% to 45.85%. After training the driving model with the 2nd round of intervention data, the performance of the model only changed a little bit since the driving model after the first round of adaptation was already reaching the efficiency constraint. Although the 2nd round of adaptation did not make big changes to the automated driving controller, it reduced the intervention rate from 45.85% to 0% since the human driver kept receiving warnings during the 1st and 2nd rounds of intervention. Overall, the proposed bilateral adaptation mechanism was able to adapt the automated driving controller to human preferences without compromising traffic efficiency, while correcting the human driver's over-conservative driving habits.

E. Robustness of Driver Model Extraction

To check the robustness and reliability of the algorithm, we compare the performance of the model learned from the original human intervention data without extra uncertainties, and the models learned from the human intervention data with injected uncertainties including both disturbances and noises. Since headway is the most important indicator of human intervention, we have injected uncertainties into such intervention data. The uncertainties are injected by adding a random value to the headway distance during a human intervention. The random value r consists of two parts, as shown in (18):

$$r = r_U + r_N, r_U \sim U(-\varepsilon, \varepsilon), r_N \sim N(0, \sigma)$$
 (18)

where r_U is a random number representing the disturbance that follows a uniform distribution between $-\varepsilon$ and ε and r_N is a random number representing the noise that follows a normal distribution with a mean value of 0 and a standard deviation of σ . r_U is generated every time a new human intervention event happens so that it can represent the disturbances of different interventions. r_N is generated every time a new human intervention data point is collected to simulate the noises within an intervention event. Then, the combined value r can become an overall representation of uncertainties in human behaviors during highway car-following.

In the first part of this section, we trained the human models when ε equals 0 and σ equals 0.3, 0.6, and 0.9 respectively to study the influence of noises, where such a noise of 0.9 is extreme for normal human intervention data. The results of trained models are shown in Fig. 8 and Fig. 9. It is shown that for both aggressive and conservative drivers, all these noise levels have little influence on the performance of the trained models. Their performance was very close to that of the one without injected noise. This indicates that our proposed approach is robust against noises during human interventions.

In the second part of this section, we trained the human models when σ equals 0.1 while ε equals 0, 3, 6, and 12 respectively, to study the influence of disturbances, where normal disturbances of human intervention data are within 6m and a disturbance of 9m is really rare. The results are shown in Fig. 10 - Fig. 12, including the statistics of differences in headway tracking performance. The results compared the models trained from the data with different levels of disturbances with the one trained with no disturbance. In the statistics charts, the blue bars represent the maximum positive headway tracking difference, the red bars represent the minimum negative tracking difference, and the lines represent the average absolute tracking difference. The data show that for both types of aggressive and conservative drivers, the disturbances did not generate noticeable differences in headway tracking performance when they are within $\pm 6m$. The disturbances have a relatively larger influence on the aggressive driver than on the conservative driver. This is because the relative value of the injected disturbance compared to the original headway is much larger for the aggressive driver. In addition, differences could be observed when

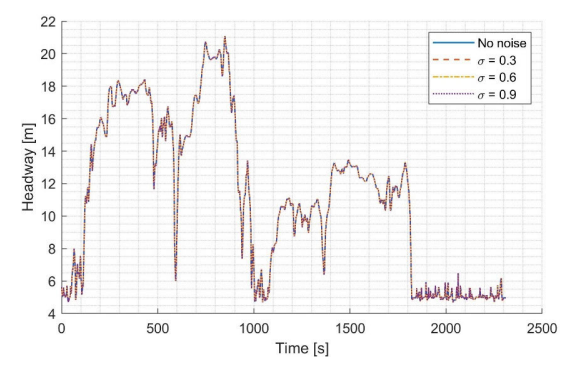


Fig. 8. Headway of models trained from data with different level of noises, aggressive driver.

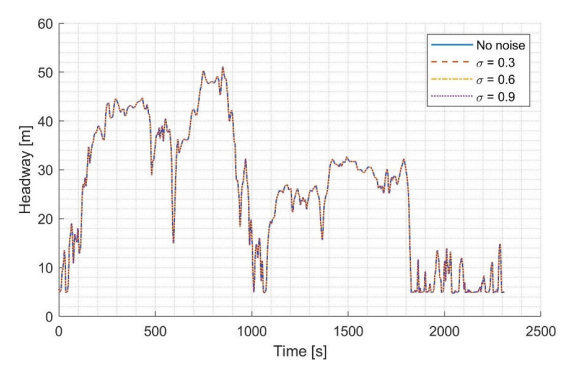


Fig. 9. Headway of models trained from data with different level of noises, conservative driver.

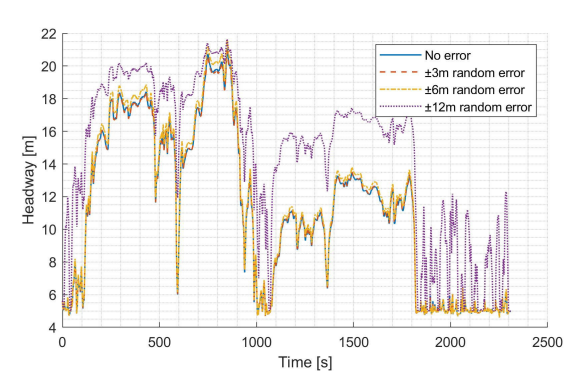


Fig. 10. Headway of models trained from data with different level of disturbances, conservative driver.

the random disturbances reach ± 12 m, especially from the aggressive driver. Such disturbances in real life mean that the aggressive driver changes his driving style by doubling, tripling, or reducing headway to a quarter frequently, which is very unlikely to happen. For the conservative driver, the difference becomes larger but is still in an acceptable range. In reality, a human driver may have some random behaviors occasionally, but in general, their driving styles should have no huge changes frequently, especially in a short period. Considering this fact, the results indicate that our proposed method is reliable and robust against disturbances during human interventions.

IV. CONCLUSION AND DISCUSSION

In this paper, a new bilateral adaptation mechanism for the longitudinal motion of automated vehicles and human drivers is proposed. The mechanism leverages the IMPC-based approach to model the generic automated driving controller and adapt it to the human drivers' preferences from the intervention data. Compared to

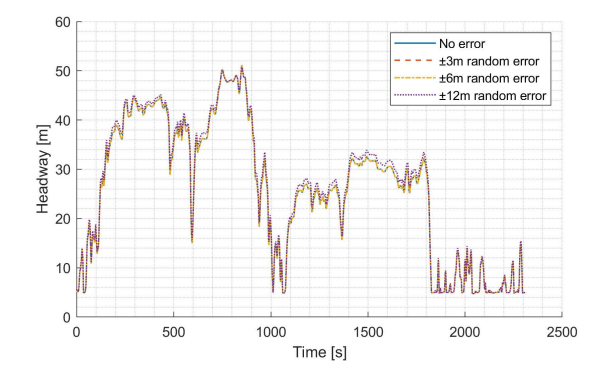


Fig. 11. Headway of models trained from data with different level of disturbances, aggressive driver.

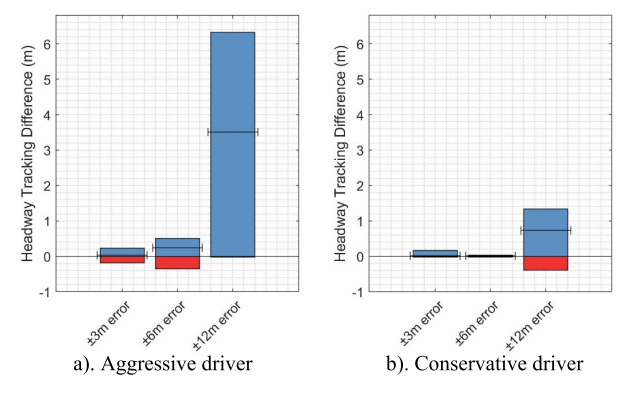


Fig. 12. Max, min and average absolute headway tracking a). Aggressive driver b). Conservative driver difference.

the one-directional adaptation methods [33], the proposed mechanism can mitigate the negative influence of improper interventions from the human driver. Moreover, the mechanism can adapt the human driver's driving habits. Human-in-the-loop experiments have been conducted in a real-time driving simulator. The experiment results show that the proposed bilateral adaptation method has achieved its design objective. A neutral automated driving controller can adapt to both aggressive and conservative driving preferences without violating safety or efficiency constraints. Human drivers can also correct their over-aggressive and over-conservative behaviors with the help of the adaptation algorithm. Nevertheless, there are some limitations to the current research work. Firstly, the existing modeling mainly focuses on the longitudinal control of the vehicle. When lateral controls are involved such as lane switching, the modeling will need to be further extended to cover the cost functions related to lateral behaviors in the future. Secondly, the current designs of the performance/safety constraints and weight selections to categorize and penalize 'unwanted' behaviors during the adaptation are a little heuristic though they work well in our studies. They can be further improved by designing more systematic and comprehensive performance/safety constraints and penalty weights based on more theoretical studies. Thirdly, the current experimental results are based on a driving simulator rather than some real vehicles to validate the designed approaches. There is a discrepancy in the human perception between the simulation and the real automated vehicle. This could lead to differences in the interventions of humans when they are sitting in a simulated automated vehicle or a real automated vehicle. Therefore, our future work is to transfer these approaches to real vehicles for actual field studies.

REFERENCES

- [1] A. M. Pereira, H. Anany, O. Pribyl, and J. Prikryl, "Automated vehicles in smart urban environment: A review," in *Proc. Smart City Symp. Prague (SCSP)*, May 2017, pp. 1–8, doi: 10.1109/SCSP.2017. 7973864
- [2] Y. Zhang, C. G. Cassandras, and A. A. Malikopoulos, "Optimal control of connected automated vehicles at urban traffic intersections: A feasibility enforcement analysis," in *Proc. Amer. Control Conf. (ACC)*, May 2017, pp. 3548–3553, doi: 10.23919/ACC.2017.7963496.
- [3] Y. Rahmati and A. Talebpour, "Towards a collaborative connected, automated driving environment: A game theory based decision framework for unprotected left turn maneuvers," in *Proc. IEEE Intell. Vehicles Symp.* (IV), Jun. 2017, pp. 1316–1321, doi: 10.1109/IVS.2017.7995894.
- [4] S. Tsugawa, S. Kato, and K. Aoki, "An automated truck platoon for energy saving," *IEEE/RSJ Int. Conf. Intell. Robots Syst.*, Dec. 2011, pp. 4109–4114, doi: 10.1109/IROS.2011.6094549.
- [5] S. Parida, M. Franz, S. Abanteriba, and S. Mallavarapu, "Autonomous driving cars: Future prospects, obstacles, user acceptance and public opinion," *Advances in Intelligent Systems and Computing*, vol. 786. 2019, pp. 318–328, doi: 10.1007/978-3-319-93885-1_29.
- [6] M. Alawadhi, J. Almazrouie, M. Kamil, and K. A. Khalil, "A systematic literature review of the factors influencing the adoption of autonomous driving," *Int. J. Syst. Assur. Eng. Manag.*, vol. 11, no. 6, pp. 1065–1082, Dec. 2020, doi: 10.1007/s13198-020-00961-4.
- [7] C. M. J. Tampère, "Human-kinetic multiclass traffic flow theory and modelling. With application to advanced driver assistance systems in congestion," Ph.D. dissertation, Dept. Civil Eng. Geosci., Delft Univ. Technol., Delft, The Netherlands, 2004.
- [8] M. Bando, K. Hasebe, A. Nakayama, A. Shibata, and Y. Sugiyama, "Dynamical model of traffic congestion and numerical simulation," *Phys. Rev. E, Stat. Phys. Plasmas Fluids Relat. Interdiscip. Top.*, vol. 51, pp. 1035–1042, Feb. 1995, doi: 10.1103/PhysRevE.51.1035.
- [9] A. Kesting and M. Treiber, "Calibrating car-following models by using trajectory data," *Transp. Res. Rec., J. Transp. Res. Board*, vol. 2088, no. 1, pp. 148–156, Jan. 2008, doi: 10.3141/2088-16.
- [10] P. Angkititrakul, C. Miyajima, and K. Takeda, "Modeling and adaptation of stochastic driver-behavior model with application to car following," in *Proc. IEEE Intell. Vehicles Symp. (IV)*, Jun. 2011, pp. 814–819.
- [11] A. Khodayari, A. Ghaffari, R. Kazemi, and R. Braunstingl, "A modified car-following model based on a neural network model of the human driver effects," *IEEE Trans. Syst., Man, Cybern. A, Syst. Humans*, vol. 42, no. 6, pp. 1440–1449, Nov. 2012, doi: 10.1109/TSMCA.2012.2192262.
- [12] J. Morton, T. A. Wheeler, and M. J. Kochenderfer, "Analysis of recurrent neural networks for probabilistic modeling of driver behavior," *IEEE Trans. Intell. Transp. Syst.*, vol. 18, no. 5, pp. 1289–1298, May 2017, doi: 10.1109/TITS.2016.2603007.
- [13] T. Gindele, S. Brechtel, and R. Dillmann, "A probabilistic model for estimating driver behaviors and vehicle trajectories in traffic environments," in *Proc. 13th Int. IEEE Conf. Intell. Transp. Syst.*, Sep. 2010, pp. 1625–1631, doi: 10.1109/ITSC.2010.5625262.
- [14] T. Kumagai and M. Akamatsu, "Prediction of human driving behavior using dynamic Bayesian networks," *IEICE Trans. Inf. Syst.*, vol. 89, no. 2, pp. 857–860, Feb. 2006, doi: 10.1093/ietisy/ e89-d.2.857.
- [15] Z. Wang et al., "Driver behavior modeling using game engine and real vehicle: A learning-based approach," *IEEE Trans. Intell. Veh.*, vol. 5, no. 4, pp. 738–749, Dec. 2020, doi: 10.1109/TIV.2020.2991948.
- [16] F. Bella and R. Russo, "A collision warning system for rear-end collision: A driving simulator study," *Proc. Social Behav. Sci.*, vol. 20, pp. 676–686, Jan. 2011, doi: 10.1016/J.SBSPRO.2011.08.075.
- [17] K. Suzuki and H. Jansson, "An analysis of driver's steering behaviour during auditory or haptic warnings for the designing of lane departure warning system," *JSAE Rev.*, vol. 24, no. 1, pp. 65–70, Jan. 2003, doi: 10.1016/S0389-4304(02)00247-3.

- [18] J. M. Sullivan, M. J. Flannagan, A. K. Pradhan, and S. Bao, "Literature review of behavioral adaptations to advanced driver assistance systems," AAA Found. Traffic Saf., 2016. [Online]. Available: https:// aaafoundation.org/wp-content/uploads/2017/12/BehavioralAdaptation ADAS.pdf
- [19] F. Biondi, I. Alvarez, and K.-A. Jeong, "Human–vehicle cooperation in automated driving: A multidisciplinary review and appraisal," *Int. J. Hum.–Comput. Interact.*, vol. 35, no. 11, pp. 932–946, Jul. 2019, doi: 10.1080/10447318.2018.1561792.
- [20] S. Maurer, R. Erbach, I. Kraiem, S. Kuhnert, P. Grimm, and E. Rukzio, "Designing a guardian angel: Giving an automated vehicle the possibility to override its driver," in *Proc. 10th Int. Conf. Automot. User Interfaces Interact. Veh. Appl.*, Sep. 2018, pp. 341–350, doi: 10.1145/3239060.3239078.
- [21] H. Zhu et al., "Camera calibration from very few images based on soft constraint optimization," J. Franklin Inst., vol. 357, no. 4, pp. 2561–2584, Mar. 2020, doi: 10.1016/J.JFRANKLIN.2020.02.006.
- [22] E. C. Kerrigan and J. M. Maciejowski, "Soft constraints and exact penalty functions in model predictive control," in *Proc. UKACC Int. Conf. (Control)*, 2000.
- [23] I. V. Kolmanovsky and D. P. Filev, "Stochastic optimal control of systems with soft constraints and opportunities for automotive applications," in *Proc. IEEE Int. Conf. Control Appl.*, Jul. 2009, pp. 1265–1270, doi: 10.1109/CCA.2009.5280822.
- [24] L. Guo and Y. Jia, "Modeling, learning and prediction of longitudinal behaviors of human-driven vehicles by incorporating internal human DecisionMaking process using inverse model predictive control," in Proc. IEEE/RSJ Int. Conf. Intell. Robots Syst. (IROS), Nov. 2019, pp. 5278–5283, doi: 10.1109/IROS40897.2019.8968292.
- [25] L. Guo and Y. Jia, "Inverse model predictive control (IMPC) based modeling and prediction of human-driven vehicles in mixed traffic," *IEEE Trans. Intell. Vehicles*, vol. 6, no. 3, pp. 501–512, Sep. 2021, doi: 10.1109/TIV.2020.3044281.
- [26] L. Guo and Y. Jia, "Anticipative and predictive control of automated vehicles in communication-constrained connected mixed traffic," *IEEE Trans. Intell. Transp. Syst.*, vol. 23, no. 7, pp. 7206–7219, Jul. 2021, doi: 10.1109/TITS.2021.3067282.
- [27] R. A. Dollar and A. Vahidi, "Efficient and collision-free anticipative cruise control in randomly mixed strings," *IEEE Trans. Intell. Veh.*, vol. 3, no. 4, pp. 439–452, Dec. 2018, doi: 10.1109/TIV.2018.2873895.
- [28] K. Mombaur, A. Truong, and J.-P. Laumond, "From human to humanoid locomotion—An inverse optimal control approach," *Auto. Robots*, vol. 28, no. 3, pp. 369–383, Apr. 2010, doi: 10.1007/s10514-009-9170-7.
- [29] R. M. Lewis and V. Torczon, "Pattern search algorithms for bound constrained minimization," SIAM J. Optim., vol. 9, no. 1, pp. 1082–1099, 1999.
- [30] Dynamometer Drive Schedules | U.S. EPA. Accessed: Apr. 8, 2022. [Online]. Available: https://www.epa.gov/vehicle-and-fuel-emissions-testing/dynamometer-drive-schedules
- [31] Emission Test Cycles: Common Artemis Driving Cycles (CADC). Accessed: Apr. 8, 2022. [Online]. Available: https://dieselnet.com/standards/cycles/artemis.php
- [32] B. Houska, H. J. Ferreau, and M. Diehl, "ACADO toolkit—An open-source framework for automatic control and dynamic optimization," *Optim. Control Appl. Methods*, vol. 32, no. 3, pp. 298–312, May 2011, doi: 10.1002/oca.939.
- [33] A. P. Bolduc, L. Guo, and Y. Jia, "Multimodel approach to personalized autonomous adaptive cruise control," *IEEE Trans. Intell. Vehicles*, vol. 4, no. 2, pp. 321–330, Jun. 2019, doi: 10.1109/TIV.2019.2904419.
- [34] J. Ploeg, A. F. A. Serrarens, and G. J. Heijenk, "Connect & drive: Design and evaluation of cooperative adaptive cruise control for congestion reduction," *J. Modern Transp.*, vol. 19, no. 3, pp. 207–213, Sep. 2011, doi: 10.1007/bf03325760.
- [35] T. J. Ayres, L. Li, D. Schleuning, and D. Young, "Preferred time-headway of highway drivers," in *Proc. IEEE Intell. Transp. Syst. (ITSC)*, Aug. 2001, pp. 826–829, doi: 10.1109/ITSC.2001.948767.